J. Fluid Mech. (1993), *vol.* 253, *pp.* 245–265

The impact of a shock wave on porous compressible foams

By B. W. SKEWS, M. D. ATKINS AND M. W. SEITZ
School of Mechanical Engineering, University of the Witwatersrand, PO WITS 2050, South Africa

(Received 24 April 1992 and in revised form 9 February 1993)

A phenomenological study of the processes occurring when a shock wave interacts with porous polyester and polyether foams has been undertaken. Plane shock waves generated in a shock tube were reflected off a slab of foam mounted against the back wall of the tube. Tests were conducted with an initial shock wave Mach number of 1.4 and a 70 mm thick slab of foam. The reduction in reflected shock wave strength and substantial increase in the back wall pressure over that for rigid wall reflection, found by other workers, were confirmed.

Piezoelectric pressure transducers were used to record the pressure before, alongside and behind the foam specimen. Schlieren photographs of the flow were made and showed some features not previously reported. In particular it is shown that there is a flow of gas across the face of the foam at some point of the process. Previous investigations of this interaction process have assumed that the face of the foam is a contact surface.

Short duration photographs of the distortion of the foam were taken, enabling the wave propagation in the foam material itself to be studied. It is established that the front of this compaction wave in the foam material moves at considerably lower velocity (~ 90 m/s) than the gas wave as detected by the pressure transducers (~ 200 m/s). This result contrasts with the assumption made in previous work that the two-phase medium behaves essentially as a homogeneous substance.

A simple physical model based on a zone of compacted material in the foam acting as a high-resistance flow barrier, is proposed to explain the observed phenomena.

1. Introduction

The study of the interaction of shock waves with porous materials has to a large extent been prompted by the need to find ways to ameliorate the effects of blast on structures and within ducts, resulting, for example, from accidental explosions. Both rigid and compressible lattice structures have been considered as attenuating media. Studies of the interaction of shock waves with porous compressible foams have shown a number of interesting features, notably that if they are attached to a rigid wall the pressure on the wall can be significantly larger than if no foam were present. Monti (1970) established the initial framework, specifically dealing with foams, in his general treatment of shock wave reflection from deformable materials. His study concentrated on the strength of the wave reflected off the front face but did indicate that backwall pressures could exceed those obtained from reflection off a rigid wall. Gelfand & Gubin (1975) measured these back wall pressures over a range of foam properties, incident shock Mach numbers, and foam lengths. They established the magnitudes of the pressure amplification that can be achieved, and ascribed the increase in pressure to the

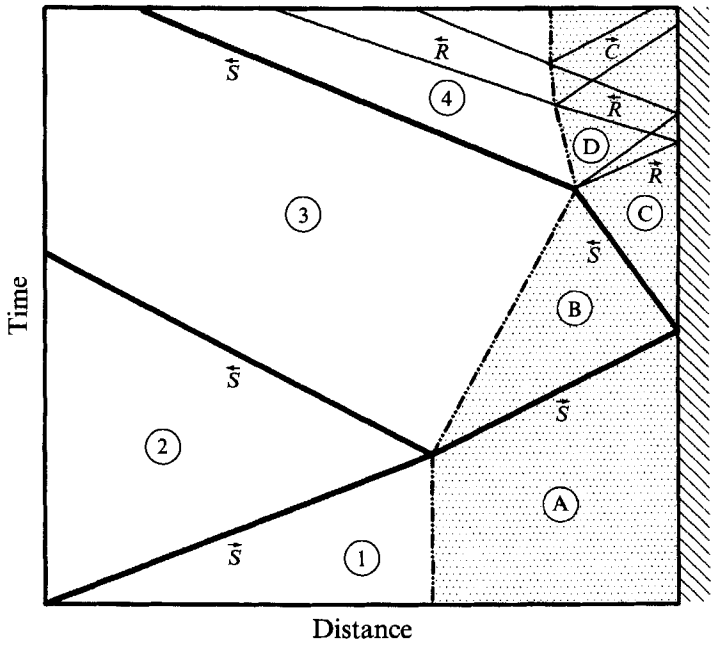

FIGURE 1. The simple refraction model.

momentum imparted to the foam by the shock wave, being subsequently transferred to the back wall. A number of experimental and theoretical studies have been undertaken since then (e.g. Gelfand, Gubanov & Timofeev 1983; Gvozdeva *et al.* 1986; Henderson *et al.* 1989). A review of much of this material has recently been given by Korobienikov (1989).

The common wave diagram model considered by all these workers is the simple refraction model shown in figure 1. Here the initial impact results in a reflected shock wave back into the gas and a transmitted shock into the foam. This latter wave reflects as a shock off the rear wall and returns to strike the foam/gas interface resulting in a shock wave transmitted into the gas and a reflected expansion wave back into the foam. This expansion wave then reflects off the back wall resulting in a reduction of pressure. Most work to date has concentrated on the high pressures developed on the back wall, although Skews (1991) has analysed the pressure field in front of the foam.

Inherent in this simple refraction model are the assumptions that there is no gas flow across the front face of the foam, that the material in the space occupied by the foam behaves as a homogeneous medium (pseudo-gas), and that the waves separate regions with uniform properties. Analytical models have been primarily based on this model. The two-phase medium is treated as a single-phase pseudo-gas with an adiabatic exponent and sound speed determined only from the ratio of the specific heats between the foam material and the gas, the ratio of the mass of gas to foam skeleton material, and the adiabatic exponent and sound speed of the interstitial gas. The details may be found in Korobeinikov (1989). The situation thus reduces to that of one-dimensional refraction of a shock wave at a gaseous interface, and may be treated using standard gas dynamic relations, with the boundary conditions of matching gas velocities and pressures across the interface. Predictions for the peak pressure on the back wall and the first reflected shock wave have been satisfactory for incident Mach numbers less than 1.6.

A recent study by Henderson *et al.* (1989), using long foam specimens (1600 mm) showed that the initial transmitted compression wave in the foam, as measured by pressure transducers, was not a shock wave, but a band of compressions becoming less steep with time. Analysis of stress/strain measurements showed that the material could be behaving in a retrograde fashion (see Thompson & Lambrakis 1973) at low stresses and strains, which they suggested could account for this effect.

Recently Baer (1992) has used continuum mixture theory to construct a numerical model to describe this interaction. He modelled the physical experiments reported by Skews (1991) and found excellent agreement with the measured pressure histories. His model also shows the existence of the compaction wave propagating through the foam skeleton, which has been shown experimentally to exist (Skews, Atkins & Seitz 1991).

The current investigation is intended to explore the phenomenological aspects of the physical behaviour and to examine the validity of the assumptions made in the refraction model. Previous studies (Gelfand *et al.* 1983; Gvozdeva *et al.* 1986; Korobeinikov 1989; Skews 1991) have shown a smooth variation of parameters with Mach number without any indication of a basic change in the process with Mach number. For this reason these detailed tests are confined to a single Mach number ($M = 1.4$). Further work will be required to find the functional dependance of the various parameters with Mach number, and such tests are currently underway. Korobeinikov (1989) has shown that the shape of the pressure pulse on the back wall is similar as the foam length changes, although the peak pressure increases as the thickness of the layer increases up to about 80 mm whereas it stabilizes at an approximately constant level, depending on the material type and the initial conditions of the experiment. The current tests were conducted with a foam length of 70 mm, which is considered to be representative for establishing the primary mechanisms of the process. This paper is an extension of material presented at the 18th International Symposium on Shock Waves (Skews *et al.* 1991; Seitz & Skews 1991).

2. Experimental facilities

The experiments were carried out in a shock tube having a compression chamber 2 m in length and an expansion chamber 5 m long. Figure 2 shows the location of the piezoelectric pressure transducers (PCB 113A21, 1 μs risetime) in the test section. Measurement resolution is better than 5 kPa, and the transducer response is linear over the range tested. Incident shock wave arrival at transducer T1 is taken as the zero reference of time for all tests. The data from the transducers was recorded by a data acquisition system sampling at 250 kHz per channel, giving time measurement accurate to 2 μs. The test section, which has a cross-section of 76.2 mm × 76.2 mm, is enclosed by two circular plate glass windows. Channel pressure for all tests was local ambient pressure (nominally 83 kPa).

Schlieren photographs were taken using a five-channel spark light source system with variable time delays between channels. For photography of the foam motion all five channels were flashed simultaneously to give sufficient light to illuminate the foam. A reflective grid of diagonal lines forming squares was painted on the side surface of the foam so that in successive photographs the path of individual points on the foam could be tracked. These short duration photographs of the foam motion will be referred to as path photographs. Details of all the schlieren and path tests undertaken, as well as the experimental arrangements are given by Atkins (1992).

Two porous compressible foams were tested: a polyether foam having a density of 32.5 kg/m^3 and a polyester foam having a density of 38 kg/m^3. The porosity coefficient

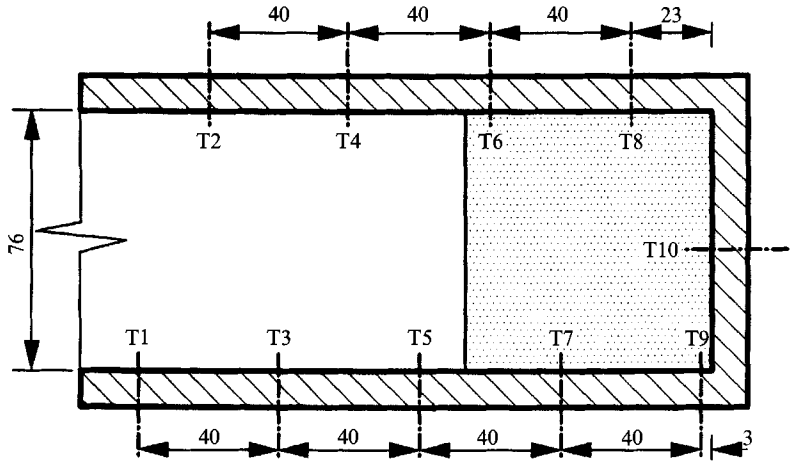

FIGURE 2. Location of the pressure transducers.

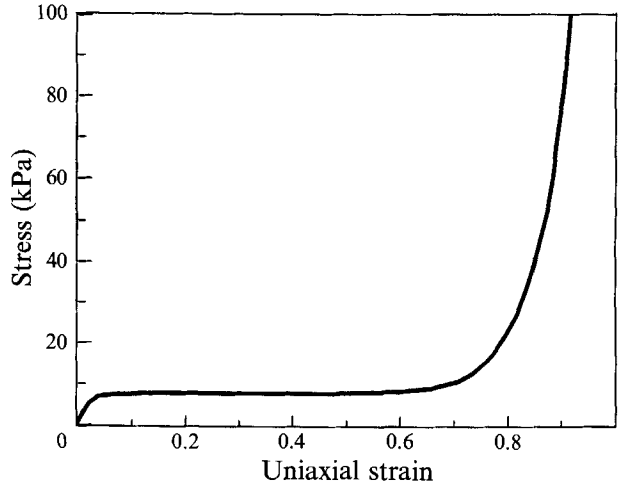

FIGURE 3. Typical deformation behaviour of open-cell polyurethane foam, $\rho = 30$ kg/m^3.

(void fraction) was about 0.98. These are both open-cell foams as defined by Gibson & Ashby (1988), which allow passage of gas from one cell to the next. The general shape of the stress–strain curve for these materials is indicated in figure 3. The curve shows a small region of linear elasticity at low stresses followed by a long collapse plateau at nearly constant stress during which the cell walls buckle, and finally a densification region where the stress rises sharply as the cell walls contact each other. The stress in the plateau region is typically less than 10 kPa for deformations of up to 70% (Monti 1970; Henderson *et al.* 1989). As will be shown later deformations of this magnitude are typical in the compaction wave.

A question which arose was whether the foam sample should fill the entire cross-section of the tube or whether a small gap should be left around the periphery to avoid wall friction. Monti (1970) used a gap and commented on the effects of non-perfect blocking and applied a correction to account for this effect. Initial tests conducted in the current study led to the decision to make the foam a slight interference fit in the

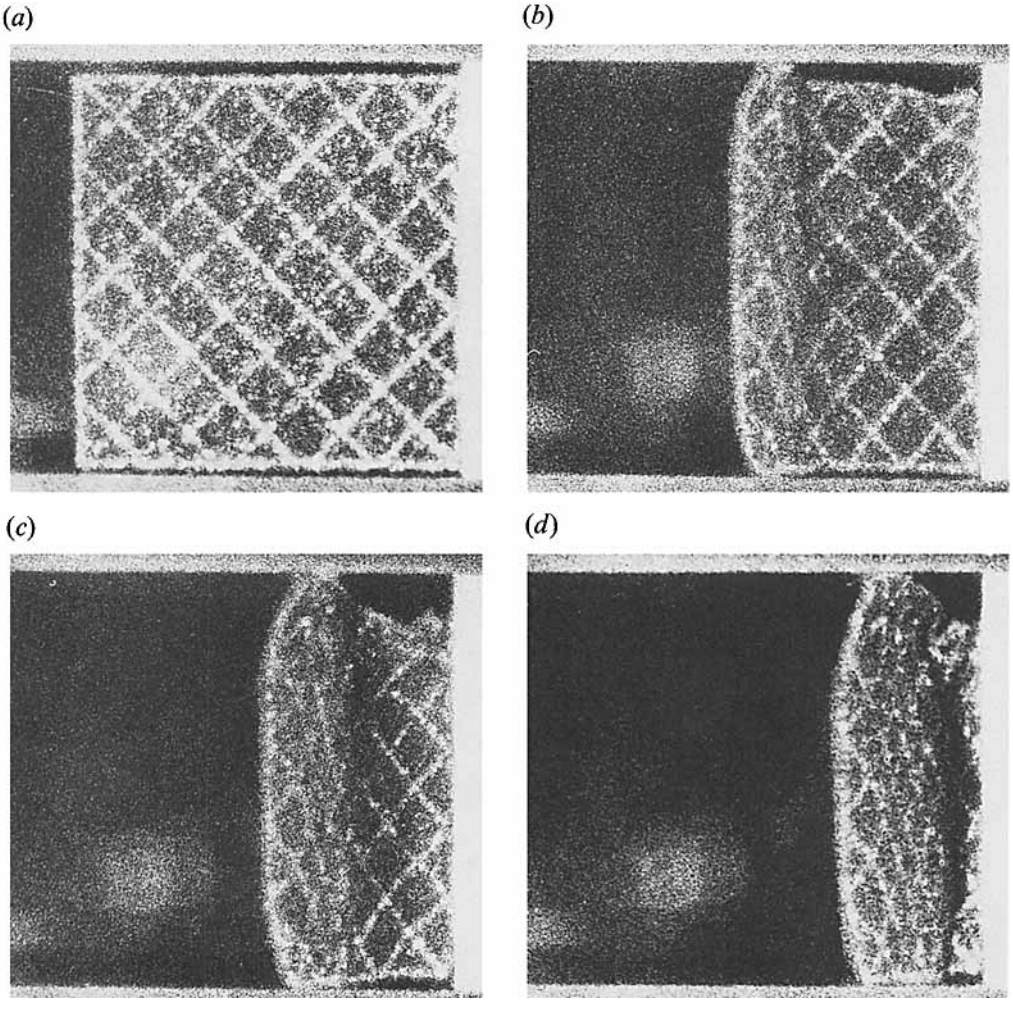

FIGURE 4. Photographs of foam collapse with an initial wall gap.

tube. Otherwise a shock wave is found to propagate through the gap and this could have affected the conclusion of some workers that a shock wave propagates through the foam. A gap certainly results in a motion further removed from one-dimensionality as is evidenced by significant lateral motion of the foam. Figure 4 shows the path photographs of a foam with an initial 2 mm gap before impact and as it collapses. The initial lateral motion of the foam is exacerbated by the development of a plug at the leading edge which serves to trap gas resulting in further lateral movement and buckling of the surface. These photographs should be compared with those of figure 5 where there is no gap. Here the foam remains adjacent to the wall over most of its length, although some distortions are noted, particularly the folding forward of the foam in the corners of the tube. The consequences of the effect of friction are evident in these photographs and will be dealt with later. The foam slab was made to slide easily into the tube in the uncompressed state. Although the Poisson's ratio is small (Monti quotes a figure of 0.01) the wall drag would be expected to increase as the foam compresses.

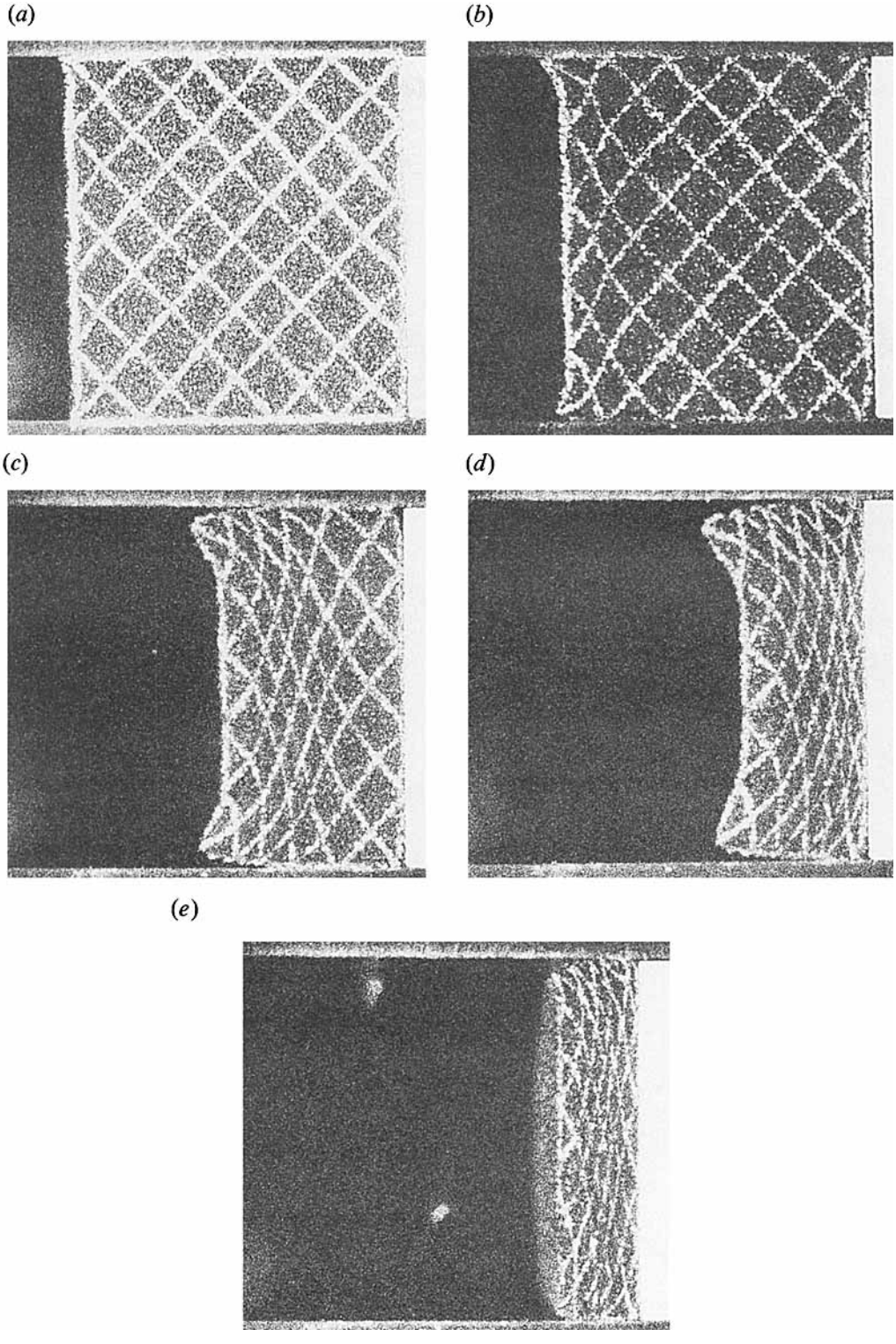

FIGURE 5. Path photographs showing foam collapse.

3. Experimental results

3.1. *Motion of the foam skeleton*

Full sets of path photographs were taken for both foams. The first photograph was taken just before the incident shock wave struck the foam and was followed by photographs at 60 μs intervals. The five photographs shown in figure 5 are part of the set taken during tests on the polyester foam.

Figure 5(*a*) shows the initial undisturbed position of the foam. The position of the diagonal lines before loading serves as a master against which subsequent motions can be measured. In figure 5(*b*), taken at 440 μs, the foam has been compressed to 60 mm. From the position of the intersection points of the lines and the distortion of the squares, the location of a wave at the front portion of foam may be identified. Figure 5(*c*) was taken at 800 μs, the foam length being 38 mm. The wave in the foam can clearly be seen, located near the centre of the reduced foam length. The front 10 mm of the foam appears to have expanded, although it is still moving down the tube. The rear half of the foam has not yet been affected, confirming that a wave of compression is propagating through the foam. It is noted that the wave is plane over most of its height, some distortion being noted towards the edges. Figure 5(*d*) shows the compaction wave having struck the rear wall of the tube resulting in the diamond shaped markings narrowing even further as the wave is reflected. Figure 5(*e*), taken at 1400 μs, shows the foam having passed its maximum compression, expanding back up the tube. The resolution of the lines is such that meaningful measurement is no longer feasible. The bulge of the centre of the foam is evident showing that the foam in contact with the wall is lagging.

In order to estimate the effects of deviation from one-dimensionality of the foam motion, primarily due to the effects of wall friction, a series of oblique photographs were taken. Figure 6 shows a typical result. As the foam compresses the front face becomes concave owing to the effects of the drag of the wall. The effects are more pronounced in the first 10 mm adjacent to the wall, the centre portion of the foam face remaining essentially plane. It should also be noted that the front 8 mm or so of the edges of the foam are folded forward and remain relatively uncompressed during the compression phase. The apparent relaxing of the foam noted before from the path photographs thus appears to be an edge effect and the material on the centreline may be fully compressed. After coming to rest at the end of the compression phase the foam starts recovering with the centre relaxing more rapidly than the edges. This results in the convex front face noted earlier. Reconstructing the oblique (perspective view) photographs into orthographic views enables an estimate to be made of the amount of dishing, so that corrections can be applied to the schlieren and path photographs in order to obtain a more realistic estimate of the foam front position on the centreline of the tube (Seitz & Skews 1991).

In view of the above, the question arises as to the validity of pressure measurements taken on the sidewall, measurements within the foam being difficult since the presence of a transducer would itself affect the foam collapse, unless it were extremely small. Although the extent of lateral pressure gradients have not been quantified they appear to be small for a number of reasons. First, in the current tests, transducer T9 is situated in the sidewall only 3 mm from the backwall and transducer T10 is in the centre of the backwall. The difference in the pressures recorded by these two transducers would thus give an indication of the lateral pressure gradient near the back wall during the early stages of the motion when the longitudinal gradient is not large. The differences in the pressures measured by these two transducers is of the order of 5% when the foam has

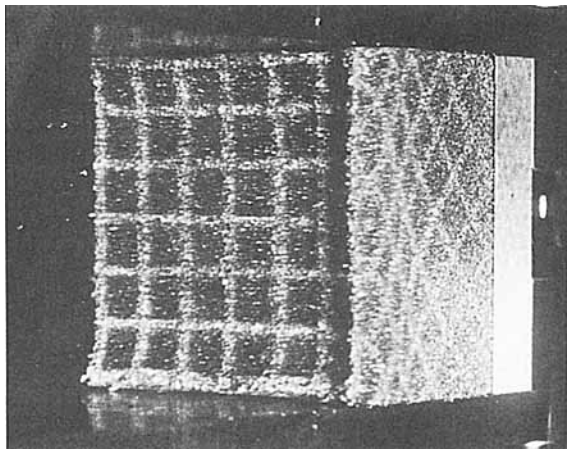

FIGURE 6. Oblique view of collapsing foam. The endwall is on the right, and the distortion of the diagonal grid lines on the side of the specimen show the compaction wave.

been compressed to half its original length. Secondly, the one-dimensional calculations of Baer (1992) give excellent agreement with the experimental results. Finally recent tests in a 180 mm high shock tube with a number of transducers distributed over the back wall also show the transverse gradients to be small. It thus appears reasonable to use sidewall measurements to infer the overall nature of the interaction.

3.2. *Schlieren photographs*

Schlieren photographs taken at the same time intervals as the path photographs, were used to establish the presence of any gas dynamic effects in front of the foam plug. Figure 7 was taken after the incident shock wave had struck the foam and shows the reflected shock wave travelling back down the tube. The reflected wave is planar. The front face of the foam is beginning to move towards the back plate, with an initial indication of the drag of the foam material in the tube corners. This causes weak transverse waves to be propagated into the flow.

For tests up to 1250 μs no gas dynamic effects are discernible, although, as will be shown later, at 1100 μs a reflected compression wave is emerging from the foam.

Figure 8, taken at 1160 μs while the foam is still being compressed, shows gas being expelled with a strongly turbulent structure. Studies using powder as a flow visualization medium (Seitz & Skews 1991) showed that this gas was being ejected at the edges of the foam, presumably resulting from the less compressed material adjacent to the wall giving a lower resistance to flow. This flow appears not to extend around the full periphery of the tube, being apparently blanked off in the corners of the tube. Shortly after these jets appear a sharp fronted disturbance emerges from the foam face. This disturbance is shown in figure 9(*a*), taken at 1400 μs. The foam has a length of 16 mm and has started to expand back up the tube. This disturbance does not reach the wall but curls up into vortices. Figure 9(*b*) was taken at 1580 μs, with the foam having a length of 22 mm. The disturbance is a well-defined discontinuity in the flow. To aid in interpretation of these photographs, a schematic representation is given in figure 9(*d*).

At the time figure 9(*c*) was taken (1880 μs) the disturbance is less clearly defined and it subsequently disappears in the turbulent background. At this stage the foam and other features are all nearly stationary.

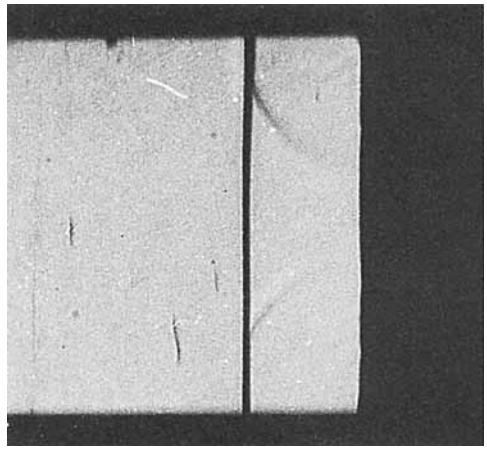

FIGURE 7. Shock wave reflection from the foam surface.

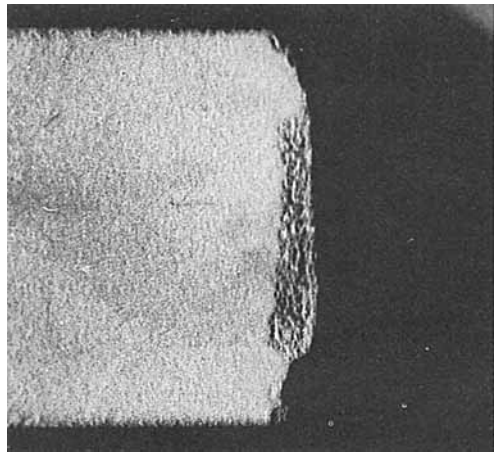

FIGURE 8. Emergence of the sidewall jets. The textured pattern in the centre of the photograph are the jets on the glass sidewalls. The top and lower wall jets are largely obscured by the folding forward of the corners of the foam.

3.3. *Pressure measurements*

Figure 10 is a typical pressure trace obtained from transducer T4, located in front of the polyester foam. The first rise in pressure is due to the incident shock wave passing the transducer. The shock wave then strikes the foam and a shock wave is reflected, giving the second rise in pressure. A compression wave followed by a weak expansion wave travelling away from the foam is subsequently recorded. These latter two waves correspond to those on either side of region 4 in figure 1. The theoretical curve for the case of a shock wave reflecting from the rigid back wall of the shock tube with no foam present is shown for comparison. It is noted that the presence of the foam in front of a solid wall significantly reduces the reflected shock wave strength and the peak pressure reached is higher than that for rigid wall reflection. The magnitude of these differences has been dealt with by Gelfand *et al.* (1983), Korobeinikov (1989) and Skews (1991).

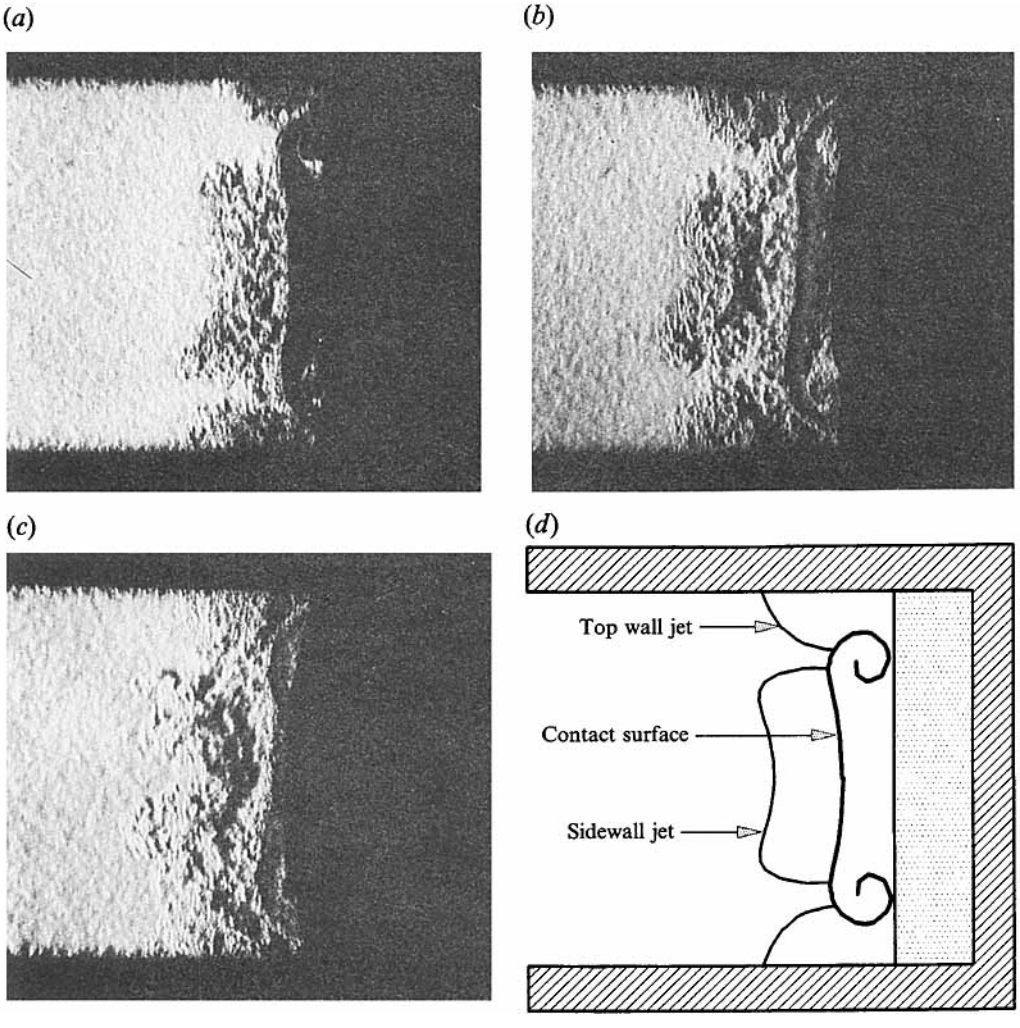

FIGURE 9. The contact surface emerging from the foam showing roll-up at the edges. It is preceded by the turbulent wall jets.

Figure 11 shows the pressure variation obtained from transducer T7, mounted alongside the polyester foam. Also shown is the theoretical trace with no foam present. The first point of note is that the measured pressure starts to rise before that expected with no foam, indicating that the transmitted wave initially moves faster than the incident wave. The spreading out of the wave as noted previously by Henderson *et al.* (1989) is also evident. However the arrival of the reflected wave is considerably delayed indicating deceleration of the wave as it moves through the foam. This matter is dealt with in greater detail in §4. It should be noted that the front face of the foam passes over this transducer position as the foam is compressed. The time at which this occurs is indicated by an arrow. To the right of this arrow the transducer is thus measuring pressure in the gas upstream of the foam face and the trace in this region is almost identical to that for transducer T4. The results for the polyether foam are very similar although the magnitudes of the pressures are somewhat lower.

Figure 12 is the trace obtained from transducer T10, situated in the back wall of the

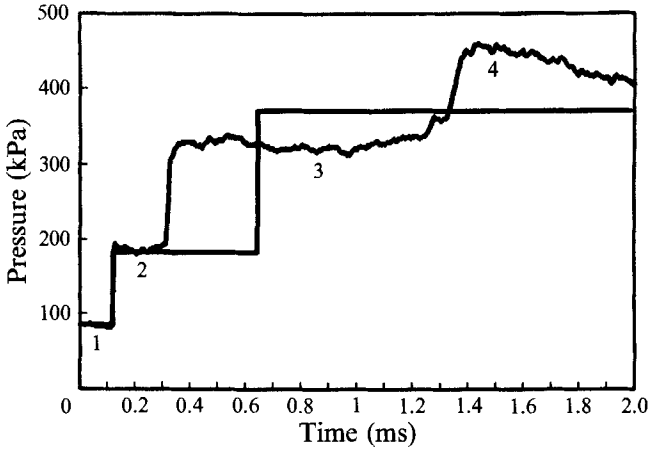

FIGURE 10. Pressure record for position T4. The straight line stepped trace is the theoretical prediction with no foam present. Symbols refer to the state of the gas as identified in figure 1.

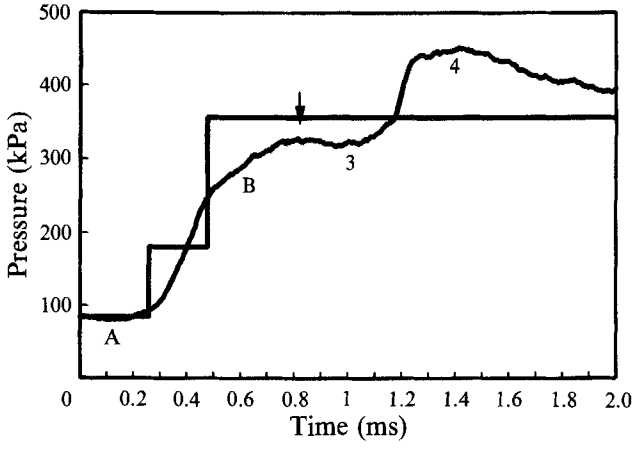

FIGURE 11. Pressure record for position T7. The straight line stepped trace is the theoretical prediction with no foam present. Symbols refer to the state of the gas as identified in figure 1.

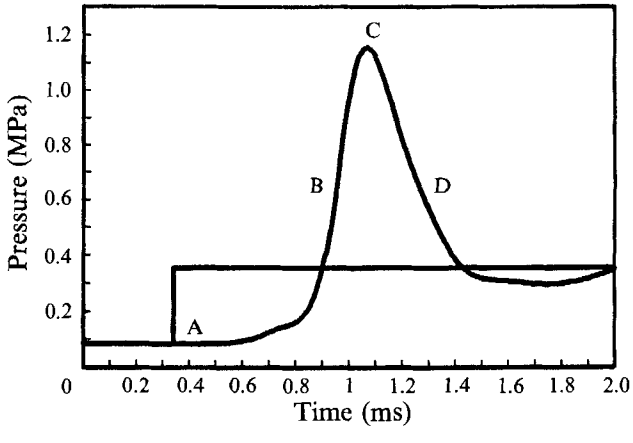

FIGURE 12. Pressure record for position T10. The straight line stepped trace is the theoretical prediction with no foam present. Symbols refer to the state of the gas as identified in figure 1.

shock tube, compared with the theoretical pressure variation with no foam. Unlike in figure 11 the start of the rise in pressure on the back wall is considerably delayed, confirming that the pressure surge through the foam is decelerating as it moves through the material. The pressure behind the reflected shock wave for rigid wall reflection is about 350 kPa compared to a pressure of 1150 kPa for the polyester foam. The foam thus acts to increase the reflected wave pressure to some considerable extent, as previously established by Gelfand & Gubin (1975), and others. For the polyether foam, the maximum back wall pressure was 750 kPa.

Using all ten transducer locations a complete pressure history throughout the test section was obtained.

4. Discussion

Each of the three different types of measurement: pressure, schlieren photography and path photography contribute to an assessment of what is happening in the foam. The experimental results for each are analysed below, and are then combined into a consistent description of the physical process.

For each path photograph the position of the intersection points of the diagonal lines in the centre portion of the foam were measured and the points originally in the same vertical plane averaged. The path of ten different planes in the foam were tracked. Figure 13 shows these paths for the polyether foam during the first millisecond of the compression stage, unfortunately, measurements at later times become suspect because the cross-over points of the painted lines become difficult to discern (figure 5). After an initial acceleration the particles travel at constant velocity. The paths clearly show the propagation of a compaction wave in the foam material; the estimated position of the head of the wave is superimposed on the figure. There is a region of highly compacted material, of increasing width, following behind this wave. The velocity of the wave front is estimated as indicated in figure 13 and is about 90 m/s for both the polyether and the polyester foam.

The position of the foam front, gas jet front and discontinuity were measured from each schlieren photograph. Figure 14 is a distance–time graph showing the motion of these interfaces for both foams tested. That of the foam front is consistent with the measurements from the path photographs. The incident shock wave strikes the foam at 190 μs, then after an initial period of acceleration the foam front moves at a constant velocity during this loading phase. The polyether and polyester foam fronts travel at 58 m/s and 54 m/s, respectively. Notwithstanding its higher density, the polyester foam accelerates to this velocity much quicker than the polyether foam. This is probably partly due to the slightly higher pressure behind the reflected shock wave and partly to the conditions influencing the initial inflow of gas, such as pore size and the flow drag characteristics of the skeleton. Tests over a wider range of conditions would be needed to explain this effect satisfactorily. The foam front then decelerates and reaches its maximum compression, polyether foam at 15 mm and polyester foam at 13 mm. The front of the edge jets emerge from the foam at considerable relative velocity, before the foam reaches the position of maximum compression, and then slow down and eventually become stationary. In looking for a one-dimensional model to describe the foam behaviour, the effects of this edge flow will be assumed to be small on the centreline flow, at least for the times under consideration. Shortly after the emergence of the edge jets the sharp-fronted disturbance emerges. This will be shown later to be a contact surface. The velocity at which it emerges from the foam cannot be determined from these results because of the concave shape of the foam front

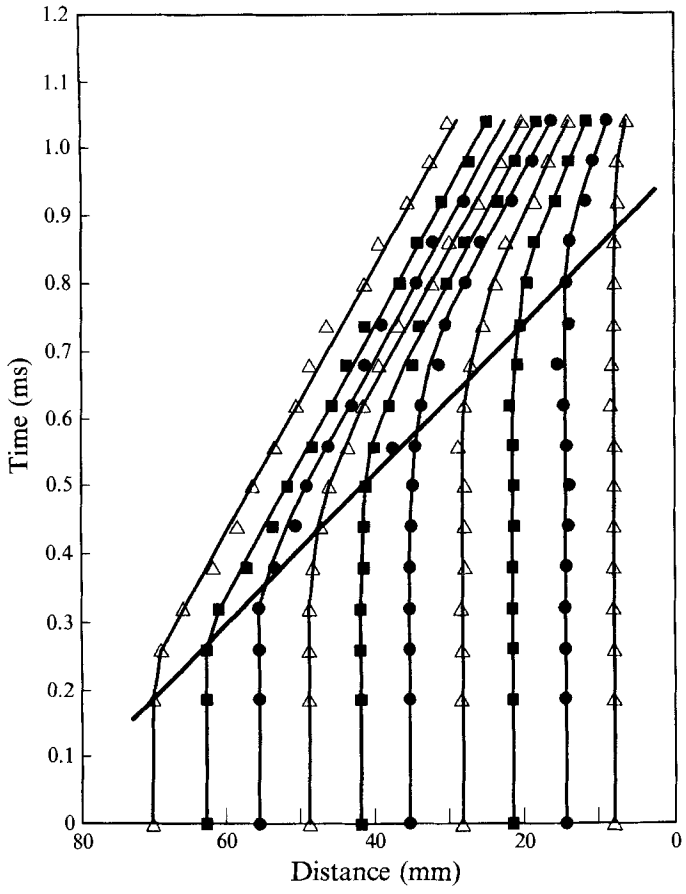

FIGURE 13. The motion of the foam skeleton. Experimental points are obtained from grid-line intersection points on the path photographs.

shielding the schlieren beam from seeing the centre of the foam. It also slows down and there is some indication that the distance between it and the foam face reduces. As will be shown later, this occurs while the flow is expanding, and it therefore implies that gas is re-entering the foam. More exact measurements will be needed to confirm this. The contact surface is no longer visible after 1.8 ms, being lost in the turbulent background.

Using all the pressure traces that were recorded, a (smoothed) contour plot, shown in figure 15, was constructed. The movement of the foam face, as determined from the path photographs, has been superimposed. This plot clearly illustrates the spreading out of the compression wave C_A transmitted into the foam. This compression wave strikes the solid wall behind the foam and is reflected as a compression C_B. The reflected compression wave then strikes the foam/air interface, resulting in a compression C_3 being transmitted into the air ahead of the foam and a rarefaction wave R_C being reflected back into the foam. This expansion reflects off the back wall giving rise to the rarefaction R_D which on reflection off the foam face results in the transmitted rarefaction wave R_4. The compression wave C_3 steepens as it propagates upstream and eventually becomes a shock wave.

The coefficient of pressure decrease of the reflected shock wave, as defined by Korobeinikov (1989), is $K = P_2/P_{20}$ where P_2 is the pressure behind the reflected shock

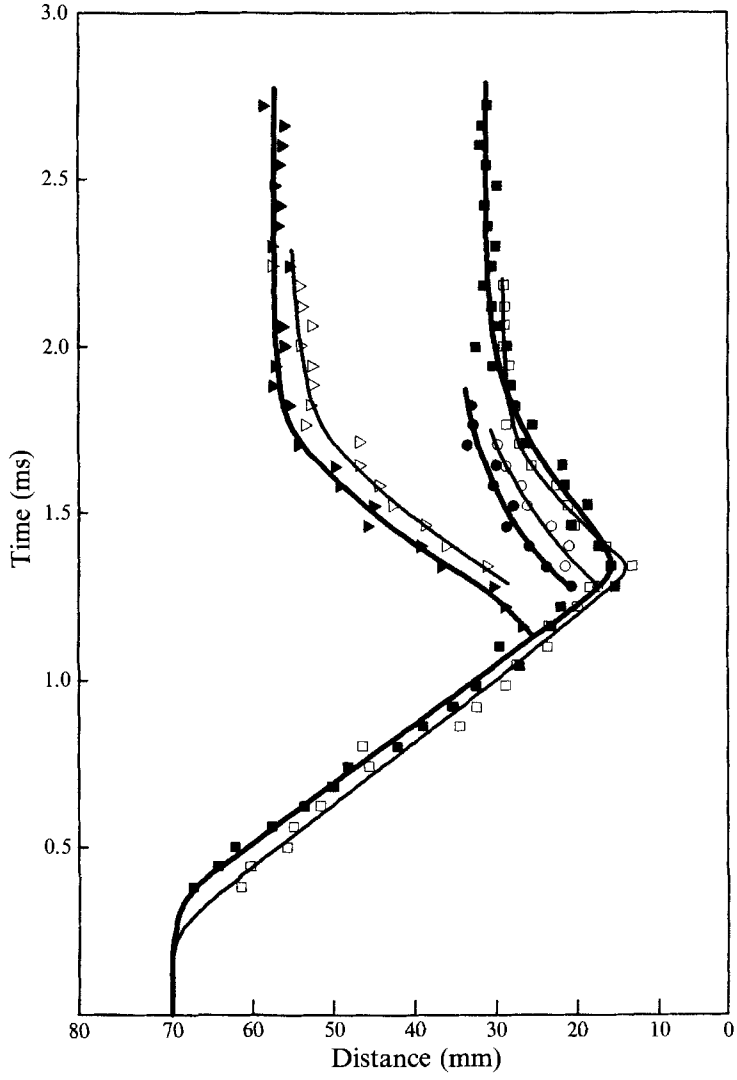

FIGURE 14. Trajectories of the main features. Solid symbols, polyether; open symbols, polyester; squares, foam front; circles, contact surface; triangles, gas jet.

wave S_2 and P_{20} is the pressure behind a shock wave reflected from a rigid wall. $K = 0.88$ for the polyether foam and $K = 0.82$ for the polyester foam. These values are similar to those given by other workers for corresponding foam densities.

The coefficient of pressure increase on the rear wall, as defined by Korobeinikov (1989), is $R_1 = P_3/P_{20}$ where P_3 is the maximum pressure reached on the rear wall behind the foam. For the present tests $R_1 = 2.5$ for the polyether foam and $R_1 = 3,1$ for the polyester foam. The peak pressure P_3 occurs before the foam reaches its maximum compression. Again these are similar to previously published results.

It is not possible to determine accurately the velocity of the leading edge of the wave measured by the pressure transducers, because of the slow initial rate of rise of the signal (figure 11). However, an examination of the pressure data files, leads to an average value of about 200 m/s. The actual value would be expected to be faster than

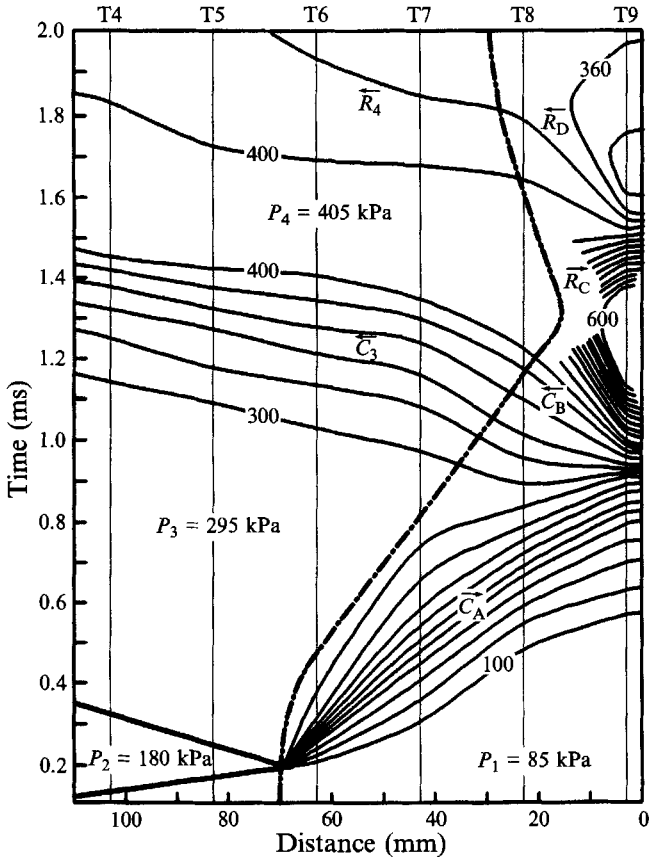

FIGURE 15. Pressure contour plot.

this but the resolution of the instrumentation does not allow this to be picked up, measurements using ultrasensitive microphones which could also withstand the peak shock pressures would be needed to do this. The average velocity of propagation of the 100 kPa contour is 180 m/s. The main point is that the gas surge moves at more than double the speed of the compression wave in the foam material. There is also evidence of this wave slowing down as it moves through the foam (see §3.3) and much more detailed measurements would need to be taken to quantify this effect. The existence of two discrete waves indicates that modelling of the process should include the separate behaviour of both phases, and treatments assuming the air/foam material to behave as a homogeneous material will not describe the process adequately. This calls for some comment on the success of the simple refraction model in predicting the strength of the first reflected wave (Skews 1991), it having now been established that the wave behaviour within the foam is rather more complex than this model allows. During the early stages of the motion each foam element is compressed to roughly half its original length as can be seen from the path photographs and figure 13. This means that it is stressed uniaxially to the level of the plateau on the stress–strain curve, to some 10 kPa above the surrounding gas pressure which is about 300 kPa. The contribution of the material elasticity is thus small and the system behaviour is dictated by the gas elasticity, as assumed in the pseudo-gas model. This reasoning was originally advanced by Gvozdeva in justifying the use of the pseudo-gas model.

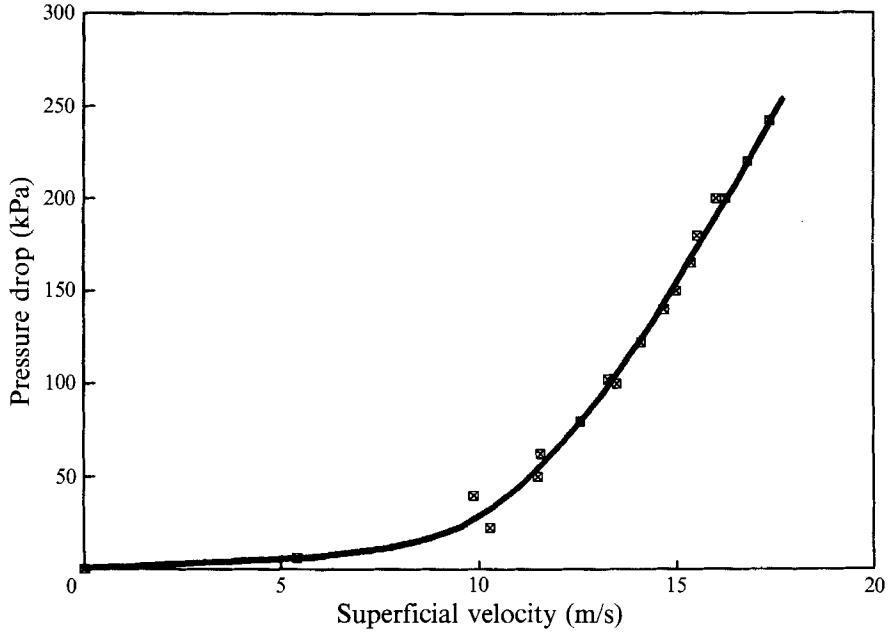

FIGURE 16. Steady flow pressure drop.

The following simple physical explanation of the processes occurring is suggested, in order to explain the observed phenomena.

It is clear that as the foam compresses, its porosity will decrease, since the change of volume is primarily due to reduction in void volume rather than that of the skeleton. Of relevance, then, is the effect this has on resistance to flow, as from the above results it is clear that there is relative motion between the gas and the surrounding skeleton. To obtain some idea of this effect a 100 mm sample of foam ($\rho = 35$ kg/m^3) supported at the downstream end against a piece of honeycomb was placed in a circular pipe. Air at different pressures was supplied upstream and exhausted to atmosphere through the foam. The mean superficial air velocity at exit was measured with a vane anemometer. The results are given in figure 16. Up to a supply pressure of some 20 kPa the flow increases gradually with pressure but then the foam starts to collapse at the downstream end and the pressure drop increases rapidly as the pores close up. (For some tests with less dense foam than dealt with in this work the velocity reaches a maximum and may even decrease as the pressure increases.) The foam plug does not collapse uniformly and even at the highest pressures employed about 80% on the upstream side remained almost fully expanded. It was unfortunately not possible with the rig used to obtain the variation of local foam density with local pressure gradient. It is clear, however, that variable flow resistance plays a major role in the behaviour of foam impacted by a shock wave.

As the shock strikes the foam some gas will flow in as the foam material accelerates but the high pressure gradient will result in pore collapse and a dramatic increase in flow resistance. (Some evidence of gas inflow during the early stages of the process has previously been given by Skews 1991.) The wave of compressed material will thus largely isolate the gas in the foam from that in front of the foam. This is supported by the finding that the foam face moves at approximately the gas velocity ahead of the foam. The advancing compaction wave may thus be considered as a piston, with some

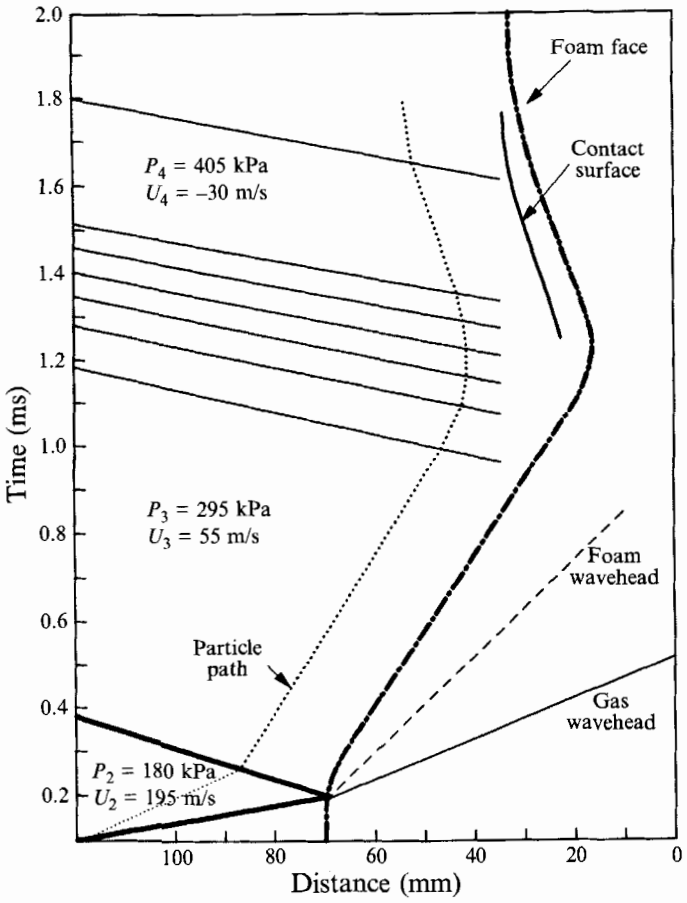

FIGURE 17. Idealized wave diagram.

leakage, depending on the pressure gradient across it, driving gas ahead of it into the foam skeleton accompanied by the associated pressure gradients. It is suggested that it is this pressure drop that is primarily responsible for the spreading out of the transmitted wave. Whilst the drag of this flow could be expected to cause some foam movement, this is masked by the drag at the wall, although some of the paths in figure 13 do show an indication of such motion.

At the end of the tube this surge of gas will be stopped and the compression wave will be reflected back into the foam thereby increasing the pressure on the back wall. The pressure gradient reverses and becomes much larger (see figure 15), both because of the increased pressure difference and the shorter length of foam. This gradient drives the hot compressed gas back out through the foam material resulting in the contact surface which is visible in the schlieren photographs.

An idealized one-dimensional representation of all the experimental results is given in figure 17. The foam path in this figure is corrected for the estimated amount of bowing of the foam face as determined from the oblique photographs. The characteristics making up the compression and expansion waves in the gas ahead of the foam are positioned according to the pressure contour plot. A calculated particle path using one-dimensional gas dynamic theory is shown for these conditions ahead of the

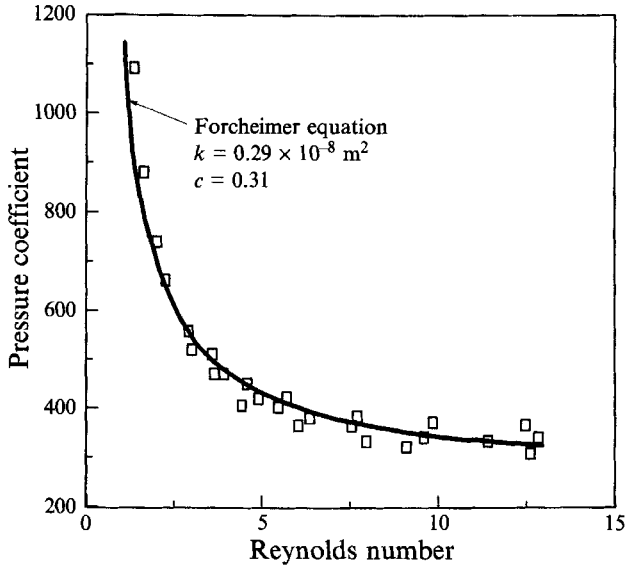

FIGURE 18. Non-dimensional pressure drop (Baer, private communication).

foam. It is noted that the path of the sharp-edged front emerging from the foam has the same slope as the particle path in region 4, thus confirming that it is a contact surface. Unfortunately the velocity, and exact time, at which it emerges from the face could not be established because of the curvature of the foam face. A more detailed series of oblique photographs will be required to do this.

Whilst the current description of the processes occurring appears adequate in explaining the observed phenomena, it is important to explore the main similarity parameters. In view of the excellent agreement obtained by Baer's (1992) mixture theory with the experimental results of Skews (1991), this theory gives a good insight into the pertinent parameters. Details of the theoretical basis for this model are given in Baer & Nunziato (1986).

The importance of the pressure drop due to flow through the skeleton is a central factor in distinguishing the current model from previous proposals. For one-dimensional flow through a porous medium this may be represented by the Forcheimer equation relating the longitudinal pressure gradient to the relative velocity (Collins 1976),

$$\frac{\Delta p}{\delta} = \frac{\mu}{k} V + \frac{c\rho}{k^{\frac{1}{2}}} V^2,$$

where k, μ and ρ are the permeability, fluid viscosity, and fluid density, and c is the inertial coefficient. Defining a Reynolds number based on the permeability as $Re = \rho V k^{\frac{1}{2}}/\mu$, gives the pressure coefficient $C_p = 2\Delta p/\rho V^2$ as

$$C_p = \frac{2c\delta}{k^{\frac{1}{2}}} + \frac{2\delta}{k^{\frac{1}{2}} Re}.$$

Steady state tests conducted by Baer (1991, private communication) on a polyurethane material similar to that used in the current tests gave the results shown in figure 18, indicating that the Forcheimer equation satisfactorily describes pressure gradients in these materials. These tests were conducted with superficial flow velocities below 5 m/s,

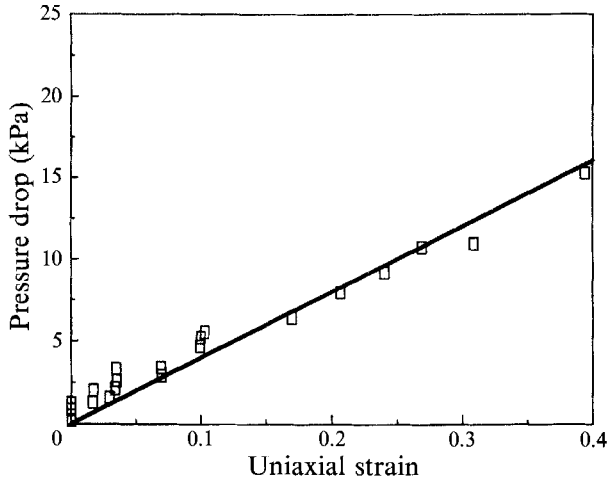

FIGURE 19. Effect of strain on pressure drop (Baer, private communication).

but were in the plateau region of the stress–strain curve. Detailed studies of the coefficients in the Forcheimer equation under varying strain conditions and with different foams, still need to be undertaken to establish the degree to which the morphology of the foam structure influences the pressure drop.

To evaluate the mechanical properties of the foam Baer (1991, private communication) examined the variation of pressure drop with uniaxial strain by measuring the reduction in length of a short specimen of foam as the pressure difference across it was increased. For a low density open cell polyurethane foam the results given in figure 19 were obtained. A linear data trend is evident. From this, the effective yield stress of the solid material may be determined, corresponding to the plateau region of the stress–strain curve. This region extends from a few per cent of strain up to some 70%. It is noted from the distortion of the grids in the path photographs and figure 13, that during the constant velocity foam compression phase the deformation is below the upper limit and a constant effective uniaxial stress in the compaction wave may be assumed. This limitation was applied in Baer's (1992) calculations. However, as the wave is brought to rest against the back wall considerably more compaction occurs and the densification phase of the stress–strain curve would be reached. Furthermore, in cases where the elasticities of the fluid and solid phase are closer to each other than in the present tests the full stress–strain relationship would need to be included, probably with the inclusion of strain rate effects.

No measurements have yet been reported on thermal effects. Gvozdeva *et al.* (1986) have shown that their experimental results lie midway between isothermal and adiabatic conditions predicted using a pseudo-gas theory considering the foam to be a homogeneous mixture of the two phases. They conclude that heat transfer between the two phases is non-negligible. In their model, Baer & Nunziato (1986) use the convective heat transfer correlation of Gel'Perin & Ainstein (1971), and also include thermal conductivity effects using appropriate thermophysical data. The relative importance of these factors has not yet been explored.

An important aspect of the Baer & Nunziato model is the development of an evolutionary equation governing the change in solid volume fraction. It is based on the entropy inequality and requires the specification of a compaction viscosity, which is a measure of the rate at which the solid volume fraction adjusts to an equilibrium stress

state. Its value is estimated using a model similar to that posed in the kinetic theory of gases (Baer 1988).

Whilst studies, prior to 1990, on the impact of a shock wave on a porous compressible foam have taken the porosity, constituent specific heats, and possibly the stress–strain relationship as the main parameters, it is apparent that the internal boundaries and interfaces influence the thermal and mechanical response to a considerable extent.

5. Conclusion

A detailed experimental study of the flow processes occurring when a weak shock wave strikes a slab of porous compressible foam adjacent to a rigid wall has been conducted. It is shown that separate, discrete waves pass through the foam skeleton and through the gas. Furthermore there is gas flow across the face of the foam. Both of these factors highlight the inadequacies of theoretical models based on a simple refraction process. Based on this new experimental evidence suggestions are made regarding the physical processes which are occurring. Further experiments are required over a wider range of incident Mach numbers and foam types to establish whether the phenomena observed are more generally applicable. Such tests, using a more sophisticated experimental facility are underway, and the results will form the basis of future analytical and numerical modelling.

REFERENCES

ATKINS, M. D. 1993 Shock wave interaction with porous compressible foams. MSc(Eng) dissertation, University of the Witwatersrand, Johannesburg, South Africa.

BAER, M. R. 1988 Numerical studies of dynamic compaction of inert and granular materials. *J. Appl. Mech.* **55**, 36–43.

BAER, M. R. 1992 A numerical study of shock wave reflections on low density foam. *Shock Waves* **2**, 121–124.

BAER, M. R. & NUNZIATO, J. W. 1986 A two-phase mixture theory for the deflagration-to-detonation transition (DDT) in reactive granular materials. *Intl J. Multiphase Flow* **12**, 861–889.

COLLINS, R. E. 1976 *Flow of Fluids through Porous Materials.* Tulsa, Oklahoma: Penn Well Publishers.

GELFAND, B. E., GUBANOV, A. V. & TIMOFEEV, A. I. 1983 Interaction of shock waves in air with a porous screen. *Isv. Akad. Nauk SSSR, Mekh. Zhid. i Gaza* **4**, 85–92.

GELFAND, B. E. & GUBIN, S. A. 1975 Study of special features of propagation and reflection of pressure waves in porous medium. *Sov. Phys., Appl. Maths Tech. Phys.* **6**, 74–77.

GEL'PERIN, N. I. & AINSTEIN, V. G. 1971 Heat transfer in fluidised beds. In *Fluidisation.* Academic Press, Berkeley, CA.

GIBSON, L. J. & ASHBY, M. 1988 *Cellular Solids – Structure and Properties.* Pergamon.

GVOZDEVA, L. G., FARESOV, Y. M., BROSSARD, J. & CHARPENTIER, N. 1986 Normal shock wave reflection on porous compressible material. *Dynamics of Explosions* (ed. J. R. Bowen, J. C. Leyer & R. I. Soloukin). Progress in Aeronautics and Astronautics 106.

HENDERSON, L. F., VIRGONA, R. J., DI, J. & GVOZDEVA, L. G. 1989 Refraction of a normal shock wave from nitrogen into polyurethane foam. *Current Topics in Shock Waves AIP Conf. Proc.* vol. 208, pp. 814–818.

KOROBEINIKOV, V. P. 1989 *Unsteady Interaction of Shock and Detonation Waves in Gases.* Hemisphere.

MONTI, R. 1970 Normal shock wave reflection on deformable walls. *Meccanica* **4**, 285–296.

SEITZ, M. W. & SKEWS, B. W. 1991 Three-dimensional effects in the study of shock wave loading of porous compressible foams. *18th Intl Symp. on Shock Waves.* Tohoku University, Sendai, Japan.

SKEWS, B. W. 1991 The reflected pressure field in the interaction of weak shock waves with a compressible foams. *Shock Waves* **1** (3), 205–211.

SKEWS, B. W., ATKINS, M. D. & SEITZ, M. W. 1991 Gas dynamic and physical behavior of compressible porous foams struck by weak shock waves. *18th Intl Symp. on Shock Waves.* Tohoku University, Sendai, Japan.

THOMPSON, P. A. & LAMBRAKIS, K. C. 1973 Negative shock waves. *J. Fluid Mech.* **60**, 187–208.